

Mixed GPS–BeiDou RTK with inter-systems bias estimation aided by CSAC

Nobuaki Kubo¹  · Hiroko Tokura¹ · Sam Pullen²

Received: 4 April 2017 / Accepted: 13 October 2017 / Published online: 4 November 2017
© Springer-Verlag GmbH Germany 2017

Abstract It is now common to use multiple GNSS constellations (multi-GNSS) for precise positioning. When GPS and BeiDou satellites are used in real-time kinematic GNSS (RTK-GNSS), the normal approach is to construct separate sets of double differences for each satellite constellation. Since QZSS is designed to be the same as GPS in terms of frequency and timing, a QZSS satellite can be used as another GPS satellite for positioning. The normal approach (“normal RTK”) requires one primary satellite for each constellation and thus removes one usable satellite. We developed a mixed GPS + BeiDou model by differencing BeiDou carrier phase and pseudorange observations from those of the primary GPS satellites. This approach introduces inter-system (GPS-to-BeiDou) biases, which must be estimated and removed. In addition, the difference between GPS and BeiDou signal frequencies means that receiver clock error has to be estimated precisely in this approach, and a chip-scale atomic clock (CSAC) was utilized to aid this estimation. The proposed mixed GPS + BeiDou RTK method was evaluated using static data and kinematic data. Kinematic data were collected in both normal and dense urban areas in Tokyo using a small car. The kinematic tests were conducted using an external CSAC as an input to the receiver, which allowed precise estimation of receiver clock error while in motion. The resulting fix rate of mixed GPS + BeiDou RTK-GNSS was approximately 10% better than normal RTK-GNSS.

Keywords RTK-GNSS · Inter-system biases · Chip-scale atomic clock · Ambiguity resolution

Introduction

The demand for accuracy and reliability of position information is increasing in location-based applications such as advanced driver assistance systems and information-oriented construction. Additionally, it is expected that the use of multiple global navigation satellite system (GNSS) constellations will expand and thus make it possible to obtain more accurate positions. The real-time kinematic (RTK) method is a relative precise positioning technique that uses observation data received at both fixed reference stations and rover stations. This technique enables us to obtain centimeter-level accuracy (Misra and Enge 2006). It is important to determine the correct integer ambiguity, and the least-squares ambiguity decorrelation adjustment (LAMBDA) method is commonly used for integer ambiguity resolution (Teunissen 1995). For correct integer ambiguity determination using the LAMBDA method, it is necessary to have a sufficient number of satellites of high measurement quality (Teunissen et al. 1999; Higuchi and Kubo 2016).

Because of the modernization of GNSS, satellite positioning systems other than the US GPS are rapidly increasing, as represented by the Russian GLONASS, the Chinese BeiDou, the European Galileo, and the Japanese Quasi Zenith Satellite System (QZSS). RTK-GNSS combines these multiple satellite systems and shows good performance in terms of both availability and accuracy in urban areas (Odolinski et al. 2015). The normal method adopted by current RTK positioning, as represented by Teunissen et al. (2014) and (Odolinski et al. (2015)), computes a single set of double differences for each satellite constellation. This choice means

✉ Nobuaki Kubo
nkubo@kaiyodai.ac.jp

¹ Tokyo University of Marine Science and Technology, Tokyo, Japan

² Stanford University, Stanford, CA, USA

that one primary satellite must be designated for each satellite constellation in order to generate double differences, and the resulting double differences are unique to each constellation. This approach is referred to as “normal RTK.”

On the other hand, double differences could instead be taken from observation data that combine satellites from different constellations. This alternative approach is called “mixed RTK.” One motivation for using mixed RTK is that only one primary satellite is required to perform the double difference for the combined set of GPS and BeiDou satellites; thus, the number of satellites that can be used for ambiguity resolution is increased by one.

In order to use mixed RTK for satellite constellations with different signal frequencies, the ISBs between different satellite constellations must be estimated. It has been reported that ISBs can reach hundreds of nanoseconds (Montenbruck et al. 2011). With respect to ISB estimation, the characteristics and calibration of ISBs between GPS (L1) and Galileo (E1) satellites, which are in the same frequency band, have been evaluated in previous research (Odijk and Teunissen 2013). However, there are still several reports on ISBs between different frequency bands. For example, the ISBs between GPS and GLONASS satellites are larger because GLONASS employs frequency-division multiple access (FDMA) (Yamada et al. 2011, 2013). In addition, BeiDou uses a different frequency than GPS, and there is a report that estimates ISBs between GPS and BeiDou satellites (Tokura and Kubo 2017).

Papers published to date on mixed RTK, such as (Tokura and Kubo 2017), mostly show results for static receivers under open-sky conditions to support theoretical algorithm evaluation. The use of mixed RTK under open-sky conditions provides no improvement over normal RTK because the performance of normal RTK is usually very good under such conditions. We change the focus to dense urban areas where an open view of the sky is not available. It examines whether the performance of mixed RTK exceeds the performance of normal RTK in terms of both availability and reliability in dense urban areas of Tokyo. Mixed RTK

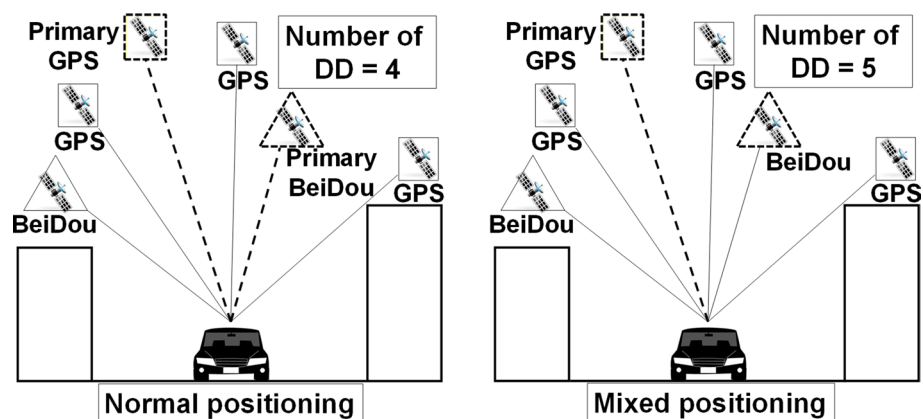
in dense urban areas presents specific challenges that were investigated and resolved, such as by adding a chip-scale atomic clock (CSAC) to estimate receiver clock error.

A mixed GPS + BeiDou model with inter-system biases (ISBs) is developed by differencing BeiDou carrier phase and pseudorange observations relative to those corresponding to the primary GPS satellite. Figure 1 shows the difference between the new mixed positioning method and the normal positioning method. In the normal positioning method, two primary satellites must be selected for GPS and BeiDou, respectively, but in the mixed positioning method, only one primary satellite is required. There are two advantages in this mixed positioning method: We can use the highest elevation satellite for the primary satellite, and the number of usable satellites for ambiguity resolution is increased.

The signal specifications of GPS and BeiDou are first introduced, and the theoretical background of ISB estimation is discussed using measurement models of pseudorange and carrier phase for GPS and BeiDou. Then, the mixed GPS + BeiDou model with ISBs is introduced, and the experiments conducted to assess its performance are described in detail. The proposed mixed GPS + BeiDou RTK method was evaluated using both static and kinematic data. The reference and rover receivers and antennas used in these tests were the Trimble NetR9 and Zephyr Model 2. ISB estimation was conducted using 12-h static data. These data were compared with ISB estimates derived from shorter periods (5 min), and the differences were very small. This comparison is important because short-period estimation will likely be needed in practical use, as receivers are sometimes restarted, which changes the ISB values. Note that dual-frequency observations were used in both normal and mixed RTK. The reason why single-frequency measurements were not sufficient is that the performance of single-frequency RTK is still not very good compared with dual-frequency RTK, especially in dense urban areas.

Kinematic data were collected in relatively open-sky condition in Tokyo. Bias estimation was conducted using the first 5 min of data, while the car was stopped under the

Fig. 1 Models of normal RTK-GNSS and mixed RTK-GNSS methods



open-sky condition. The fix rate of mixed GPS + BeiDou RTK was comparable to the fix rate of normal GPS + BeiDou RTK with separate double differences. Through this kinematic test, we found that the accuracy of receiver clock estimation was essential to the improvement of the mixed GPS + BeiDou RTK method because the frequency difference between GPS and BeiDou directly affected the accuracy of bias estimation. In the case of normal internal receiver clock stability of the receiver, it was difficult to accurately estimate receiver clock error because large, frequent jumps in the estimated clock error can be seen. These were mostly caused by two factors. The first was large dilution of precision (DOP) values due to blocked or obscured satellite signals. The second was severe multipath signals in the challenging urban environment driven in Tokyo, which includes several overpasses, tunnels, and many high-rise buildings. Therefore, two additional kinematic tests were conducted using an external chip-scale atomic clock (CSAC). The behavior of the estimated receiver clock using the CSAC was very smooth and easy to estimate. By estimating receiver clock error as accurately as possible using the CSAC and the least-squares method, the fix rate of mixed GPS + BeiDou RTK was superior to the result of normal RTK. Specifically, the fix rate was improved by approximately 10% compared with normal RTK.

Normal and mixed GPS + BeiDou RTK methods

In this section, mixed and normal RTK positioning methods are introduced, and the ISB concept is further clarified. In RTK positioning, we take the difference of observation data at the base station and the user at the same epoch in order to cancel satellite-derived errors. This method is called single difference. Single-difference methods include receiver clock bias, which is common to the single-difference measurements from all satellites at each epoch. This term can be eliminated by forming between-receiver and between-satellite double-difference measurements, which is called the double-difference method. Reference satellites for double-difference calculation are chosen based on the elevation angle: the highest elevation satellite is chosen as the primary satellite.

GPS and BeiDou signal frequencies

The signal frequencies of GPS and BeiDou are shown in Table 1. BeiDou was operating 20 satellites on three types of satellite orbits as of June 2016, when the first set of kinematic experiments was conducted. There are five satellites in geostationary orbit (GEO), eight satellites in inclined geosynchronous orbit (IGSO), and seven satellites in medium earth orbit (MEO). With five GEOs and eight IGSOs, the

Table 1 Signal frequencies of GPS and BeiDou

System	Frequency band	Center frequency (MHz)
GPS	L1	1575.420
	L2	1227.600
	L5	1176.450
BeiDou	B1	1561.098
	B2	1207.140
	B3	1268.520

increase in the number of satellites in the Asia and Oceania region is significant. A total of 31 GPS satellites are currently in operation as of June 2016. In this study, we used the following dual-frequency observation data: GPS L1 C/A, GPS L2P (semi-codeless), QZSS L1 C/A, QZSS L2C, and BeiDou B1 and B2. Table 1 shows the center frequencies of each of the GPS and BeiDou signals. Note that Japanese QZSS signals are assumed to have the same characteristics as the corresponding GPS signals. With regard to potential ISBs between GPS and QZSS, we have evaluated these for RTK several times in the past, and no measurable biases have been observed. Therefore, QZSS satellites are treated as additional GPS satellites.

Measurement model and single differences

GPS and QZSS pseudorange and carrier phase measurements are modeled as

$$P_{r,j}^s = \rho_r^s + a_{r,j}^s + c \cdot (dt_r - dt^s) + d_{r,j}^G - d_j^s + e_{r,j}^s \tag{1}$$

$$\begin{aligned} \phi_{r,j}^s = & \left(\lambda_j^s\right)^{-1} \cdot \left(\rho_r^s + \alpha_{r,j}^s + \epsilon_{r,j}^s\right) + f_j^s \cdot (dt_r - dt^s) \\ & + \delta_{r,j}^G - \delta_j^s + \varphi_{r,j} - \varphi_j^s + N_{r,j}^s \end{aligned} \tag{2}$$

The subscript r identifies a term associated with a receiver, while the subscript s identifies a term associated with a GPS or QZSS satellite. The subscript j identifies a term associated with a GPS frequency band (e.g., L1 or L2). P_j^s is the pseudorange measurement [m], ϕ_j^s is the carrier phase measurement [cycles], c is the speed of light [m/s], λ_j^s is the wavelength [m], f_j^s is the center frequency of satellite [Hz], ρ_r^s is the true range to satellite [m], $a_{r,j}^s$ and $\alpha_{r,j}^s$ are the atmospheric errors [m], dt_r and dt^s are the receiver and satellite clock errors [s], $e_{r,j}^s$ and $f_{r,j}^s$ are the receiver noise and multipath signals [m], $d_{r,j}^G$ is the receiver hardware code bias

(GPS) [m], d_j^s is the satellite hardware code bias [m], δ_{rj}^G is the receiver hardware carrier bias (GPS) [cycles], δ_j^s is the satellite hardware carrier bias [cycles], $\varphi_{r,j}, \varphi_j^s$ are the receiver initial carrier phase and satellite initial carrier phase [cycles], $N_{r,j}^s$ is the integer ambiguity [cycles].

BeiDou pseudorange measurements and carrier phase measurements are analogous to those of GPS and are modeled as follows:

$$P_{r,k}^q = \rho_r^q + a_{r,k}^q + c \cdot (dt_r - dt^q) + d_{r,k}^B - d_k^q - \text{GBTO} + e_{r,k}^q \tag{3}$$

$$\begin{aligned} \phi_{r,k}^q &= (\lambda_k^q)^{-1} \cdot (\rho_r^q + \alpha_{r,k}^q - \text{GBTO} + \epsilon_{r,k}^q) + f_k^q \cdot (dt_r - dt^q) \\ &+ \delta_{r,k}^B - \delta_k^q + \varphi_{r,k} - \varphi_{r,k}^q + N_{r,k}^q \end{aligned} \tag{4}$$

The subscript q identifies a term associated with a BeiDou satellite. The subscript k identifies a term associated with a BeiDou frequency band (e.g., B1 or B2). $d_{r,k}^B$ is the receiver hardware code bias (BeiDou) [m], $\delta_{r,k}^B$ is the receiver hardware carrier bias (BeiDou) [cycles], and GBTO is the GPS–BeiDou system time bias [m].

The receiver hardware biases (d, δ), which are the cause of inter-system biases between GPS and BeiDou, are the result of time delay differences in the circuits between the signals within a GNSS receiver and depend on signal frequency. Additionally, because each satellite constellation uses its own system time, there is a time offset between GPS and BeiDou. This time offset is defined as GBTO and is based on GPS system time. Atmospheric errors, including ionospheric and tropospheric errors, are assumed to be negligible because short baselines between reference and rover receivers are assumed.

The GPS–BeiDou single differences between base station and rover receivers can be expressed as

$$P_{rb,j}^s = \rho_{rb}^s + c \cdot (dt_{rb}) + d_{rb,j}^G + e_{rb,j}^s \tag{5}$$

$$\begin{aligned} \phi_{rb,j}^s &= (\lambda_j^s)^{-1} \cdot (\rho_{rb}^s + \epsilon_{rb,j}^s) + f_j^s \cdot (dt_{rb}) \\ &+ \delta_{rb,j}^G + \varphi_{rb,j} + N_{rb,j}^s \end{aligned} \tag{6}$$

$$P_{rb,k}^q = \rho_{rb}^q + c \cdot (dt_{rb}) + d_{rb,k}^B + e_{rb,k}^q \tag{7}$$

$$\begin{aligned} \phi_{rb,k}^q &= (\lambda_k^q)^{-1} \cdot (\rho_{rb}^q + \epsilon_{rb,k}^q) + f_k^q \cdot (dt_{rb}) \\ &+ \delta_{rb,k}^B + \varphi_{rb,k} + N_{rb,k}^q \end{aligned} \tag{8}$$

Subscripts b and r indicate terms associated with the base station or rover station, respectively. $(*)_{rb} = (*)_r - (*)_b$. This

difference eliminates the system time bias between GPS and BeiDou.

Next, to cancel the errors caused by the receiver, double-difference observations are generated. Here, two different approaches are introduced. The first approach is to separate the double differences for each satellite constellation into independent sets—one for each constellation. The other approach is to not separate the double differences for each satellite constellation, i.e., to use a mixed GPS + BeiDou model by differencing the BeiDou carrier phase and pseudorange observations relative to those corresponding a single primary GPS satellite. This approach introduces inter-system biases (ISBs) between GPS and BeiDou.

Double difference for normal RTK-GNSS

Normally, as explained above, double differences are generated separately for each constellation. The double differences for GPS and BeiDou are written separately as

$$P_{rb,j}^{s1s2} = \rho_{rb}^{s1s2} + e_{rb,j}^{s1s2} \tag{9}$$

$$\phi_{rb,j}^{s1s2} = (\lambda_j^s)^{-1} \cdot (\rho_{rb}^{s1s2} + \epsilon_{rb,j}^{s1s2}) + N_{rb,j}^{s1s2} \tag{10}$$

$$P_{rb,k}^{q1q2} = \rho_{rb}^{q1q2} + e_{rb,k}^{q1q2} \tag{11}$$

$$\phi_{rb,k}^{q1q2} = (\lambda_k^q)^{-1} \cdot (\rho_{rb}^{q1q2} + \epsilon_{rb,k}^{q1q2}) + N_{rb,k}^{q1q2} \tag{12}$$

Subscripts s1 and s2 represent GPS satellite numbers. Subscripts q1 and q2 represent BeiDou satellite numbers. $(*)_{rb}^{s1s2} = (*)_{rb}^{s1} - (*)_{rb}^{s2}$. Because the geometric distance and integer ambiguities remain in the double difference of the carrier phase measurements, the final precise position is calculated by determining the correct integer ambiguities for both GPS and BeiDou.

Double difference for mixed RTK-GNSS

Here, the double difference for mixed GPS and BeiDou is introduced. The primary satellite is set to be the GPS satellite with the highest elevation angle. The resulting double differences are (for the GPS-to-BeiDou case, the GPS-to-GPS equations are the same as for normal RTK):

$$P_{rb,jk}^{qs} = \rho_{rb}^{qs} + d_{rb,jk}^{BG} + e_{rb,jk}^{qs} \tag{13}$$

$$\begin{aligned} \phi_{rb,jk}^{qs} &= (\lambda_j^s)^{-1} \cdot (\rho_{rb}^s + \epsilon_{rb,j}^s) - (\lambda_k^q)^{-1} \cdot (\rho_{rb}^q + \epsilon_{rb,k}^q) \\ &+ (f_j^s - f_k^q) \cdot (dt_{rb}) + \delta_{rb,jk}^{BG} + N_{rb,jk}^{qs} \end{aligned} \tag{14}$$

Again, subscript s indicates a GPS satellite number, and subscript q indicates a BeiDou satellite number. The unit for code measurements is meters, and the unit of carrier measurements is cycles. Note that these mixed double differences include those for GPS satellites only, and the observation equations for those satellites are the same as in Eqs. (9) and (10).

In the double differences of the pseudorange measurements, the hardware code bias difference between reference and rover receivers remains. Because this bias is unique for each satellite constellation, we define ISB_{p1} to be the bias due to the L1–B1 pseudorange measurement in the double difference and ISB_{p2} to be the bias due to the L2–B2 pseudorange measurement in the double difference.

On the other hand, for the double differences of the carrier phase measurements, because the frequencies of GPS and BeiDou are different, the receiver clock error term remains. This receiver clock error implies that this model is even weaker than the traditional GPS + BeiDou model in Eqs. (9)–(12) without accurate estimation of the clock error. Therefore, in terms of the redundancy of the mixed model, at least dual-frequency measurements would then be needed. The details of the effect of receiver clock error on integer ambiguity resolution are discussed in a later section.

Additionally, as with pseudorange measurements, the hardware carrier bias difference between reference and rover receivers remains. We define $ISB_{\varphi1}$ for the bias due to the L1–B1 carrier phase measurement in the double difference and $ISB_{\varphi2}$ for the bias due to the L2–B2 carrier phase measurement in the double difference. Once we accurately estimate these biases and errors, the ambiguities for double differences of carrier phase measurements will remain as integers. The integer parts of $ISB_{\varphi1}$ and $ISB_{\varphi2}$ are included in the integer ambiguities, while the decimal part is estimated.

Estimation and stability of ISBs

From Eqs. (13) and (14), ISB estimation requires elimination of the term due to geometric distance. In this section, the estimation of ISBs performed using two different receivers under zero-baseline conditions is presented.

Zero-baseline test

A zero-baseline test was carried out by connecting two receivers to the same antenna. After estimating the ISBs of the pseudorange and carrier phase measurements, mixed

GPS + BeiDou RTK performance was evaluated using the estimated ISB.

A Trimble Zephyr Geodetic 2 antenna was installed on the rooftop of the building that houses our laboratory on our university campus, which has an open-sky environment. Static data were acquired for 12 h using two sets of Trimble NetR9 receivers in March 2016. Data from GPS, QZSS, and BeiDou satellites were collected and used for analysis. It is expected that the temperature change during data acquisition was small in our laboratory in March. The elevation mask angle was set to 15° . The data sampling rate was 1 Hz.

Zero-baseline test for ISB estimation

The double differences between GPS-L1 and BeiDou-B1 for the Trimble NetR9 receivers were evaluated. In addition, the double differences between GPS-L2 and BeiDou-B2 for the Trimble NetR9 receivers were evaluated. The primary satellite for double-difference calculations was selected to be the one with the highest elevation angle among the visible GPS and QZSS satellites. The average number of visible satellites was 7.7 for GPS and 7.0 for BeiDou for the NetR9 receivers.

Figures 2 and 3 show the temporal double differences of all BeiDou satellites in zero-baseline mode. Pseudorange biases are shown in the upper plot of each figure, while carrier phase biases are shown in the lower plot. Each distinct color in these plots shows the results for a particular BeiDou satellite. These figures also show the average and standard deviation of the biases over all plotted BeiDou satellites. In the case of carrier phase biases, the integer part is removed and only the decimal part is shown. The ISBs were stable for 12 h, and the standard deviation of the ISB estimates was 0.02 cycles for both L1–B1 and L2–B2. Using these results, the results of mixed GPS + BeiDou RTK experiments are discussed in the next section.

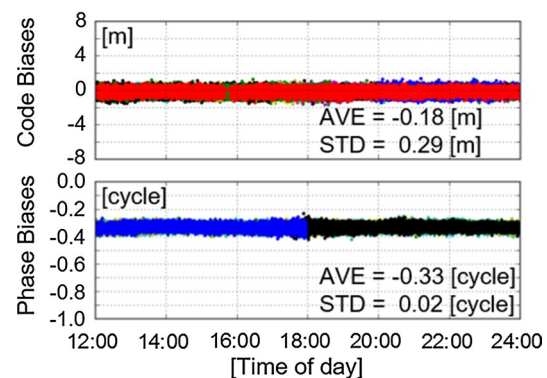


Fig. 2 Double differences between L1–B1 using NetR9 receivers (zero baseline)

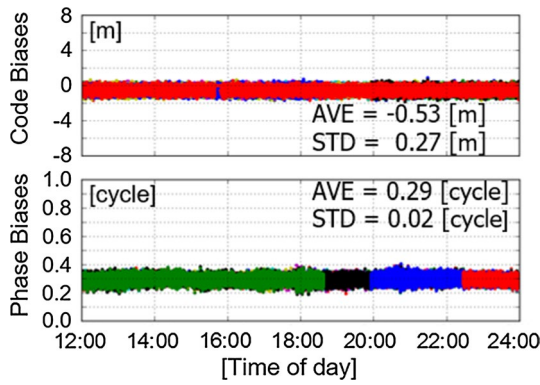


Fig. 3 Double differences between L2–B2 using NetR9 receivers (zero baseline)

Investigation of ISB estimated over a short period (5 min)

When the ISB correction method in RTK-GNSS is used for kinematic tests, the accuracy of the ISB estimated using a short period (e.g., 5 min) is important for practical use. Unfortunately, in the case of GPS + GLONASS, the estimated ISBs change once we restart the receiver (Furuya et al. 2014). We also have confirmed that the estimated ISBs for GPS + BeiDou change once we restart the receiver. For practical uses of RTK for kinematic application such as in vehicles, it is quite helpful if we can estimate and re-estimate ISBs in short periods because these applications may need to restart the receiver frequently.

The accuracy of ISB estimated using a short period was evaluated based on the 12-h average value given in the previous section. Here, the 12-h average value was treated as the reference ISB. The average of the most recent 5 min of measurements was used to estimate the temporal ISB. Figures 4 and 5 show the temporal ISB estimated using 5-min measurements for NetR9 (L1–B1 and L2–B2) receiver. The estimated average ISB using this short period for the NetR9 receiver was almost within 0.01 cycles of the 12-h average estimate at all times. These values are small enough to resolve correct ambiguities in terms of mixed GPS + BeiDou RTK.

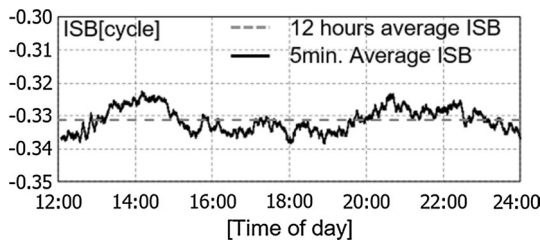


Fig. 4 12-h average ISB and the average ISB from the most recent 5 min of measurements between L1–B1 by (NetR9 receiver)

Effect of Receiver Clock Error on ISB Estimation

As can be seen from the third term in Eq. (14), correctly estimating the receiver clock error is very important because this term strongly affects the accuracy of ISB estimation. Note that standalone positioning gives us an estimate of receiver clock error at the reference station, while differential positioning gives us an estimate of the difference in receiver clock error between the rover and the reference station. To consider the effect of receiver clock error on ISB estimation, the third term of Eq. (14) for L1–B1 and L2–B2, respectively, can be written as

$$\begin{aligned}
 (f_{L1}^s - f_{B1}^q) \cdot (dt_{rb}) &= (f_{L1}^s - f_{B1}^q) \cdot (dT_{rb} \times c^{-1}) \\
 &= (1575.420 - 1561.098) \\
 &\quad \cdot 10^6 \cdot dT_{rb} \cdot (3.00 \cdot 10^8)^{-1} \\
 &= 0.048 \cdot dT_{rb}
 \end{aligned}
 \tag{15}$$

$$\begin{aligned}
 (f_{L2}^s - f_{B2}^q) \cdot (dt_{rb}) &= (f_{L2}^s - f_{B2}^q) \cdot (dT_{rb} \times c^{-1}) \\
 &= (1227.600 - 1207.140) \\
 &\quad \cdot 10^6 \times dT_{rb} \cdot (3.00 \cdot 10^8)^{-1} \\
 &= 0.068 \cdot dT_{rb}
 \end{aligned}
 \tag{16}$$

f is the center frequency of the satellite [Hz], c is the speed of light [m/s], dt_{rb} is the receiver clock error [s], and dT_{rb} is the receiver clock error [m].

These two equations show the effect of receiver clock error in units of meters. If there is a residual error of 1 m obtained from receiver clock error estimation, a bias of 0.048 cycles between L1 and B1 and 0.068 cycles between L2 and B2 will occur. Under open-sky conditions, it is not hard to estimate receiver clock error within 1 m; however, it will be difficult to consistently estimate receiver clock error within 1 m in urban areas because multipath errors and degraded DOP will affect the estimates. Under severe urban conditions, the error in the estimated receiver clock error can exceed 10 m, making it difficult to resolve inter-system ambiguities in mixed GPS + BeiDou RTK. In terms of the redundancy of the model in Eqs. (13) and (14), if we

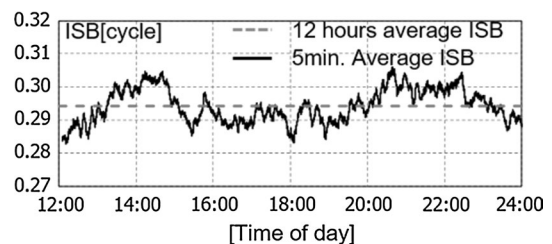


Fig. 5 12-h average ISB and the average ISB from the most recent 5 min of measurements between L2–B2 by (NetR9 receiver)

can estimate receiver clock error with sufficient accuracy, the effective redundancy increases. Otherwise, the effective redundancy does not increase, as the inaccurate clock bias estimate removes the advantage of the additional usable satellite shown in Fig. 1. To evaluate the overall performance of the mixed RTK-GNSS, actual test results are shown in the following section.

Mixed GPS + BeiDou RTK using the estimated ISBs

Using the estimated 12-h average ISB derived in the previous section, mixed GPS + BeiDou instantaneous RTK was performed using the same data described in the previous section. The baseline length was zero, and 12-h data were used. The LAMBDA method was used for ambiguity resolution, and the ratio test was used for integer ambiguity validation with a threshold value of 3. This threshold of 3 was chosen based on our previous experience in using RTK for both static and kinematic tests as well as the experience of others (Verhagen and Teunissen 2013).

Table 2 shows the test results of mixed RTK-GNSS after ISB calibration. Availability is defined as the number of epochs with fixed solutions divided by the total number of epochs. Fixed solutions mean the epochs in which integer ambiguities were successfully fixed while meeting the ratio test threshold. Reliability is defined as the number of correct fixed solutions divided by the number of fixed solutions. If the horizontal difference between the fixed position and the true position is less than 5 cm, this solution is regarded as a reliable solution. Based on these results, use of the estimated average ISB was effective. Without these ISB corrections, no fixed solutions were obtained.

Note that both availability and reliability for normal RTK using GPS + BeiDou, where ISB estimation is not required, were 100%, respectively. The LAMBDA method with the same threshold of 3 was used for normal RTK as well as for mixed RTK, and dual-frequency measurements were used in both methods.

Kinematic test for mixed GPS + BeiDou RTK method

This section presents two experimental results for mixed RTK-GNSS to evaluate performance under kinematic

conditions in urban areas. These experiments were performed in an urban environment in Tokyo, Japan, in June and December 2016. The two test routes are shown in Figs. 6 and 7. The satellite constellations during these two test periods are shown in Figs. 8 and 9. There were several short overpasses and a truss bridge that caused 2–3-s GNSS outages during the first test. There were many high-rise buildings, several overpasses, and a tunnel that caused 30–40-s GNSS outages during the second test. A geodetic-level GNSS antenna and the Trimble NetR9 receiver were used to obtain raw GNSS data using a small car. The permanent reference station on the rooftop of our laboratory building was used to produce correction data. The receiver and antenna for the reference station are Trimble NetR9 and Zephyr geodetic 2. The maximum length of the baseline between the reference station and rover car was approximately 4 km. In addition, a Microsemi Quantum™ SA.45s CSAC was connected to the rover receiver via its external frequency input to compare performance based on the accuracy and stability of the receiver clock. The CSAC provides the accuracy and stability of atomic clock technology while achieving reduced



Fig. 6 Kinematic test route in the vicinity of our university (Tsukishima, Tokyo, Japan)



Fig. 7 Kinematic test route in a dense urban area (Ginza, Tokyo, Japan)

Table 2 Results of mixed RTK method after ISB calibration

Receiver	Availability	Reliability	Horizontal standard deviation	Vertical standard deviation
NetR9	100.0%	100.0%	2.1 mm	3.8 mm

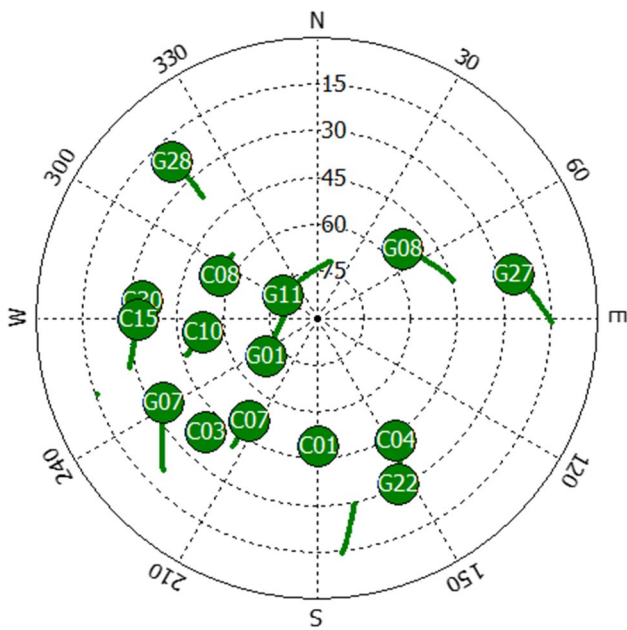


Fig. 8 Satellite constellation during the first test (June 2016)

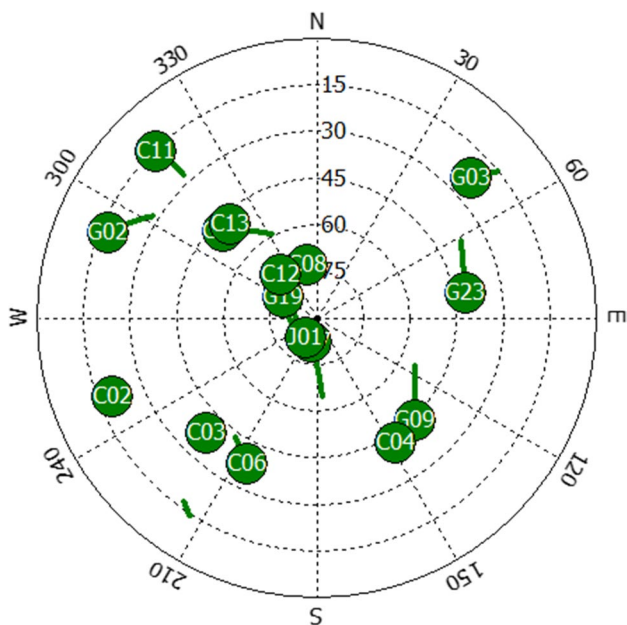


Fig. 9 Satellite constellation during the second test (December 2016)

size, weight, and power consumption. The reference positions were deduced in post-processing from the POS LVX system manufactured by Applanix Corporation for Trimble. GPS, QZSS, and BeiDou satellites were used in the analysis to investigate mixed RTK-GNSS using estimated ISBs. The duration of the tests was approximately 30 min for both tests. The sampling rate of these data was 10 Hz for the rover and 1 Hz for the reference station. The elevation mask angle was

set at 15°, and the minimum carrier-to-noise ratio was set at 30 dB-Hz for all received signals except for GPS L2P, where it is set to 20 dB-Hz.

ISB estimation during the initial test period

To evaluate mixed GPS + BeiDou RTK under kinematic conditions, the ISBs must be estimated beforehand. To do this, the rover car stopped for over 5 min under relatively open-sky conditions before it started to move. ISBs were then estimated using 5-min fixed positions as in the previous section when zero-baseline tests were conducted.

Clock offset using CSAC augmentation

Data from the first kinematic experiment in June 2016 were evaluated in terms of the clock offset with CSAC augmentation of the rover receiver. Figure 10 shows the estimated clock offset using pseudorange DGNSS of GPS + BeiDou at the rover. As can be seen from this result, there were occasionally large jumps of longer than 0.1 μs. As explained earlier regarding (15) and (16), we must attempt to keep the accuracy of the clock offset estimate within a few meters, which is equivalent to within approximately 0.01 μs. Therefore, least-squares estimation was applied to more accurately determine the temporal clock offset in the rover receiver as well as in the reference receiver. To estimate the clock offset at the current epoch, the previous 5 min of DGNSS clock offset estimates were used to calculate a least-squares fit to a 1-D line which means linear regression at every epoch. Furthermore, large outliers in the estimated clock offset were removed; specifically, differences between the predicted value using the fitted line and the observed current clock offset that exceeded 5 meters were excluded and replaced with the predicted value. To compare mixed GPS + BeiDou RTK with normal GPS + BeiDou RTK fairly, this

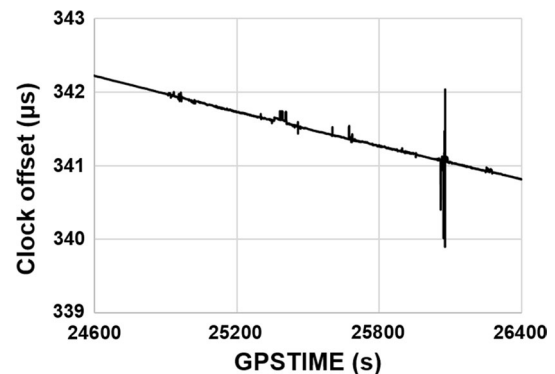


Fig. 10 Estimated receiver clock offset based on DGNSS using CSAC input (at rover)

linear regression approach to determine the clock offset was applied in both methods.

Mixed RTK and normal RTK results in the first experiment

This section compares the results for both normal RTK and mixed RTK from the first experiment. No filtering methods were applied to the float solutions for the two RTK methods, nor was the velocity derived from Doppler frequency (Kubo 2009) used. Figure 11 shows the horizontal positions provided by the normal RTK method where RTK fixes could be computed. Figure 12 shows the horizontal positions provided by the mixed RTK method where RTK fixes could be computed. The results show that the mixed RTK GPS + BeiDou method was superior in terms of the availability of fixed positions when compared to the normal RTK method. Roughly speaking, mixed RTK could successfully resolve the integer ambiguities even, while the rover is on the truss bridge, near overpasses, and close to high-rise buildings. On the other hand, the performance of both RTK methods was similar under favorable conditions, meaning no sky blockages or abnormal multipath.

Table 3 shows the availability and the reliability of these test results for both RTK methods along with the maximum interval between fixed epochs, which was investigated because the interval between precise position fixes directly affects the quality of the integration of GNSS with other sensors such as inertial measurement units. Recall that availability is defined here as the number of epochs in which fixed RTK solutions were derived divided by the total number of epochs, while reliability is defined as the number of correct fixed solutions divided by the number of fixed solutions. The total number of epochs was 16,000 at 10 Hz. The number of epochs in each result is provided in parentheses. If

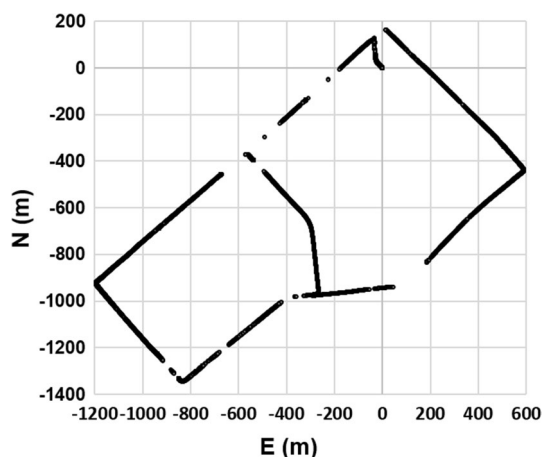


Fig. 11 Fixed horizontal positions using the normal RTK method (1st experiment)

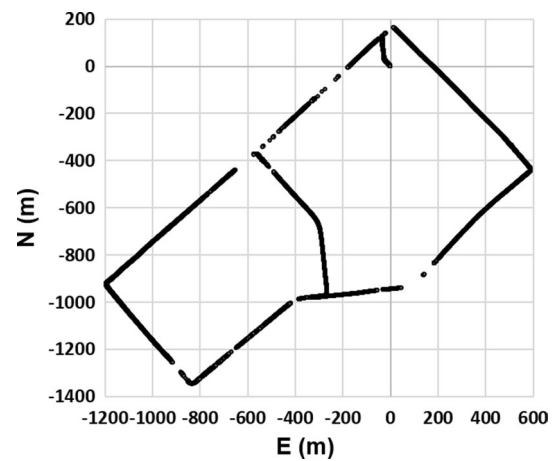


Fig. 12 Fixed horizontal positions using the mixed RTK method (1st experiment)

the horizontal difference between the fixed position and the true position determined from POS LVX is less than 20 cm, that solution is regarded as a reliable solution. The mixed RTK method performed better than the normal RTK method under all of these criteria.

Mixed RTK and normal RTK results in the second test

Finally, this section compares the results for both normal RTK and the mixed RTK from the second experiment using the same approach as in the first experiment. In this experiment, we repeated the driving route in a dense urban area three times. Figure 13 shows the horizontal positions provided by the normal RTK method where RTK fixes could be computed. Figure 14 shows the horizontal plots provided by the mixed RTK method where RTK fixes could be computed. As in the case of the second experiment, these results show that the mixed RTK GPS + BeiDou method was superior in terms of the availability of fixed positions when compared to the normal RTK method.

One key feature of mixed RTK in this test is that it successfully resolved integer ambiguities soon after exiting the long tunnel, which is illustrated in Fig. 15. The figure compares the enlarged horizontal positions during the second drive over the route near the northwest corner, which is just after the tunnel exit. The red plot shows the results of normal RTK, and the black plot shows the results of mixed RTK. Note that the black plot resumes much earlier than the red plot as the car moves from right to left after leaving the tunnel, indicating that RTK position fixes resume for mixed RTK about 160 m before they resume for normal RTK. The maximum horizontal error due to incorrect fixes was also greatly reduced from 18.10 m for normal RTK to 0.93 m for mixed RTK, as shown in Fig. 16. The figure compares the enlarged horizontal positions of the first drive over the

Table 3 Results of normal RTK method and combined RTK method after calibration of ISB using kinematic data (1st experiment)

	Availability	Reliability	Maximum interval between fixed epochs (s)
Normal RTK-GNSS	65.8% (10,520)	99.95% (10,515)	32.4
Mixed RTK-GNSS	74.2% (11,877)	100% (11,877)	20.4

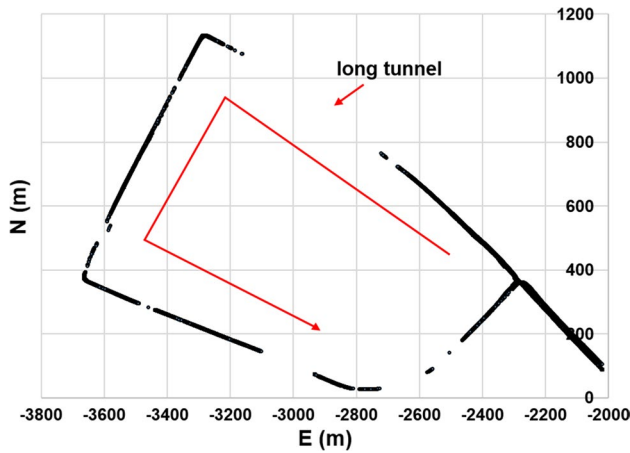


Fig. 13 Fixed horizontal positions using the normal RTK method (2nd experiment)

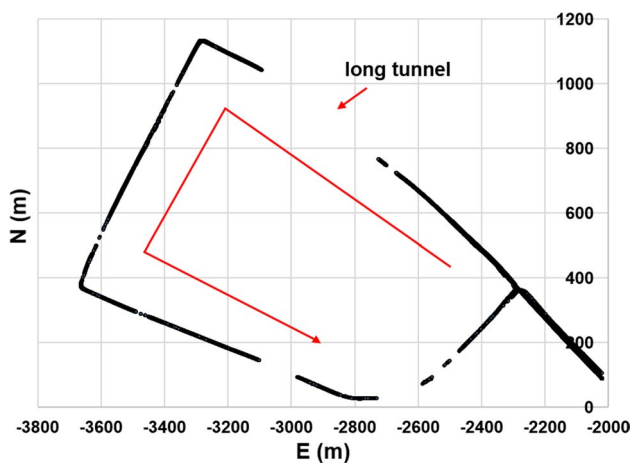


Fig. 14 Fixed horizontal positions using the mixed RTK method (2nd experiment)

route near the southwest corner. Here, normal RTK briefly produced large errors due to erroneous integer ambiguity fixes, while this did not occur for mixed RTK under the same conditions.

Table 4 shows the availability and the reliability of these test results along with the maximum interval between fixed estimates. For this experiment, the maximum interval between fixed epochs does not include the period when the rover was inside long tunnel mentioned above. The total

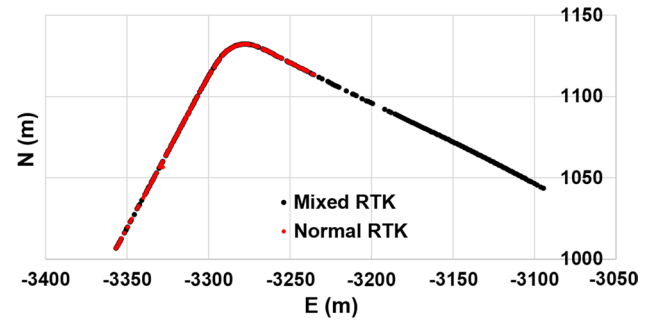


Fig. 15 Enlarged fixed horizontal positions between the normal RTK and the mixed RTK near the northwest corner of the route

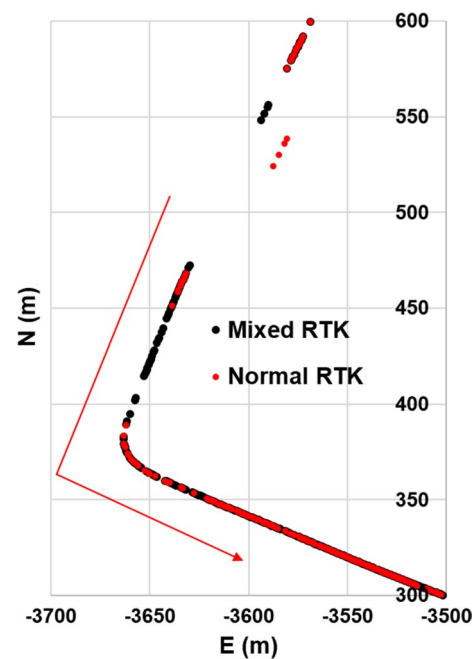


Fig. 16 Enlarged fixed horizontal positions between the normal RTK and the mixed RTK near the southwest corner

number of epochs was 20,200 at 10 Hz, including the period within the long tunnel. Again, the mixed RTK method performed better than the normal RTK method under all of these criteria. In particular, after excluding the period, while within the long tunnel, the maximum interval between fixed epochs was reduced dramatically from 43.3 to 21.4 s when using mixed RTK in place of normal RTK.

Table 4 Results of normal RTK method and combined RTK method after calibration of ISB using kinematic data (2nd experiment)

	Availability	Reliability	Maximum interval between fixed epochs (s)
Normal RTK-GNSS	56.5% (11,420)	99.89% (11,407)	43.3
Mixed RTK-GNSS	65.2% (13,165)	99.95% (13,159)	21.4

Conclusions

In RTK-GNSS, computing separate sets of double differences for each satellite constellation has become the normal approach. However, we can combine double differences for each satellite constellation if we can estimate the resulting inter-system biases (ISBs). We developed a mixed GPS + BeiDou model with inter-system biases by differencing BeiDou carrier phase and pseudorange observations relative to those corresponding to a primary GPS satellite. The proposed mixed GPS + BeiDou RTK method was evaluated using static and kinematic data. Inter-system bias estimation was conducted using 12-h data from a high-grade GNSS receiver. Mixed RTK-GNSS using the above-estimated ISBs was successful in general. The estimated ISBs were very stable over 12 h. However, we need to estimate ISBs over much shorter periods in practical use. Therefore, ISBs estimated over 12 h were compared to estimates made over a much shorter period (5 min), and the difference was small for the high-grade GNSS receiver.

The advantage of mixed RTK-GNSS is that the number of satellites that can be applied to integer ambiguity resolution is increased by reducing the number of primary satellites. Additionally, we can choose the highest satellite from any GNSS constellation in this method, which enables us to retain the same primary satellite for a longer period, even in urban areas. The key question is whether these advantages are sufficient to overcome the need for ISB estimation and the influence of ISB estimation errors.

To evaluate the performance of mixed RTK-GNSS, kinematic data were collected in both normal and dense urban areas in Tokyo during June and December 2016. ISB estimation was conducted using the first 5 min of data, while the car was stopped under open-sky conditions. Through these kinematic tests, we found that the accuracy of receiver clock estimation was essential for the mixed GPS + BeiDou RTK method because frequency differences between GPS and BeiDou directly affect the accuracy of ISB estimation. Therefore, the kinematic experiments were conducted using an external CSAC. The behavior of the estimated receiver clock using CSAC was very smooth and easy to estimate. By estimating the receiver clock error as accurately as possible using least-squares linear regression, the fix rate of mixed GPS + BeiDou RTK was superior to that of normal RTK. The proposed method improved the performance in

challenging sky view conditions. Specifically, the fix rate was improved by approximately 10%, as compared with the normal RTK method. Furthermore, the number of large errors due to wrong integer ambiguity fixes was decreased.

In future work, we will investigate the possibility of not using external clock equipment to allow for a more realistic use of RTK-GNSS in a vehicle. The possibility of using low-cost single-frequency receiver will be checked in relatively open-sky condition. We must also further investigate the stability of the estimated ISBs, which means that we must determine how ISBs depend on factors such as time, the type of receiver/antenna, and temperature.

References

- Furuya T, Sakai K, Mandokoro M, Tsuji H, Hatanaka Y, Munenaka H, Kawamoto S (2014) Development of multi-GNSS analysis software GSILIB. *J Geospat Inf Auth Jpn* 125:125–131
- Higuchi M, Kubo N (2016) Achievement of continuous decimeter-level accuracy using low-cost single-frequency receivers in urban environments. In: *Proceedings of ION GNSS 2016*, Institute of Navigation, Portland, Oregon, 12–16 Sept, pp 1891–1913
- Kubo N (2009) Advantage of velocity measurements on instantaneous RTK positioning. *GPS Solut* 13(4):271–280
- Misra P, Enge P (2006) *Global positioning system: signals, measurements and performance*, 2nd edn. Ganga-Jamuna Press, Lincoln
- Montenbruck O, Hauschild A, Hessel U (2011) Characterization of GPS/GIOVE sensor stations in the CONGO network. *GPS Solut* 15(3):193–205
- Odijk D, Teunissen PJG (2013) Characterization of between-receiver GPS-Galileo inter-system biases and their effect on mixed ambiguity resolution. *GPS Solut* 17(4):521–533
- Odolinski R, Teunissen PJG, Odijk D (2015) Combined GPS + BDS for short to long baseline RTK positioning. *Meas Sci Technol* 26(4):1–16
- Teunissen PJG (1995) The least-squares ambiguity decorrelation adjustment: a method for fast GPS integer ambiguity estimation. *J Geod* 70(1–2):65–82
- Teunissen PJG, Joosten P, Odijk D (1999) The reliability of GPS ambiguity resolution. *GPS Solut* 2(3):63–69
- Teunissen PJG, Odolinski R, Odijk D (2014) Instantaneous BeiDou + GPS RTK positioning with high cut-off elevation angles. *J Geod* 88(4):335–350
- Tokura H, Kubo N (2017) Study on inter-system biases estimation for combined GPS-BeiDou RTK-GNSS. *Inst Electron Inf Commun Eng B* 100(3):291–299
- Verhagen S, Teunissen PJG (2013) The ratio test for future GNSS ambiguity resolution. *GPS Solut* 17(4):535–548

Yamada H, Takasu T, Kubo N, Yasuda A (2011) Evaluation of positioning performance for RTK-GPS/GLONASS with calibrated inter-channel hardware biases. *Trans Navig* 124:103–110

Yamada H, Takasu T, Sakai T, Kubo N, Yasuda A (2013) Calibration of inter-channel biases on GLONASS signals. *Inst Electron Inf Commun Eng B* 96(7):793–801



Nobuaki Kubo received his Master's degree in Electrical Engineering in 1998 from Hokkaido University. He received his doctorate in Engineering from the University of Tokyo in 2005. He resided at Stanford University in 2008 as a visiting scholar. He is now an associate professor at the Tokyo University of Marine Science and Technology (TUMSAT), specializing in GPS/GNSS systems. His current interests are high-accuracy automobile navigation using RTK and multipath mitigation

techniques.



Hiroko Tokura has received her Doctoral degree in Engineering in 2017 from the TUMSAT in Tokyo. She is now a software engineer at NEC Aerospace Systems Ltd. Her current interest is high-accuracy positioning using multiple GNSS satellite constellations (multi-GNSS).



Sam Pullen is the technical manager of the ground-based augmentation system (GBAS) research effort at Stanford University, where he received his Ph.D. in Aeronautics and Astronautics in 1996. He has supported the FAA and other service providers in developing system concepts, technical requirements, integrity algorithms, and performance models for GBAS, SBAS, and other GNSS applications and has published well over 100 research papers and articles. He has also

provided extensive technical support on GNSS, its applications, system optimization, and risk assessment through his consultancy, Sam Pullen Consulting. He was awarded the ION Early Achievement Award in 1999 and was elected an ION Fellow in 2017.